Received: 19 January 2022 | Revised: 26 February 2022 | Accepted: 28 February 2022

DOI: 10.1002/ddr.21939

RESEARCH ARTICLE

DRUG DEVELOPMENT RESEARCH WILEY

Secoisolariciresinol diglucoside induces pyroptosis by activating caspase-1 to cleave GSDMD in colorectal cancer cells

Tuo Chen[1,2] | Zhen Wang[3] | Junbo Zhong[1] | Lijun Zhang[4] | Haopeng Zhang[5] | Dayong Zhang[6] | Xiaofeng Xu[6] | Xianfei Zhong[3] | Jing Wang[7] | Hai Li[2]

[1]Department of Burn and Plastic Surgery, Zigong Fourth People's Hospital, Zigong, Sichuan, China

[2]Department of Colorectal Surgery, General Hospital of Ningxia Medical University, Yinchuan, Ningxia, China

[3]Department of Gastroenterology, The People's Hospital of Leshan, Leshan, Sichuan, China

[4]Respiratory and Critical Care Medicine, Yanzhou Branch of Affiliated Hospital of Jining Medical University, Jining, China

[5]School of Clinical Medicine, Ningxia Medical University, Yinchuan, China

[6]Department of Urinary Surgery, Zigong Fourth People's Hospital, Zigong, Sichuan, China

[7]Xi'an Medical University School of Stomatolog, Xi'an, Shanxi, China

Correspondence

Hai Li, Department of Colorectal Surgery, General Hospital of Ningxia Medical University, Yinchuan, Ningxia, China.
Email: ctbaby2021@163.com

Zhen Wang, Department of Gastroenterology, The People's Hospital of Leshan, Leshan, Sichuan, China.
Email: sciwangzhen@163.com.

Funding information

National Natural Science Foundation of China, Grant/Award Number: 81960526

Abstract

Secoisolariciresinol diglucoside (SDG) is the main component of lignans with various biological activities, including anticancer activity. However, whether SDG has obvious anticancer effects on colorectal cancer (CRC) is unclear. Pyroptosis, a form of programmed cell death, has received increasing attention in cancer-related research. In this study, we aimed to test the anticancer properties and relatecd functional mechanisms of SDG. we found that SDG not only inhibited the cell viability of HCT116 cells, but also induced HCT116 cells to swell with apparent large bubbles, which are typical signs of pyroptosis. Furthermore, SDG induced cell pyroptosis by enhancing cleavage of the N-terminal fragment of gasdermin D (GSDMD) in CRC cells, accompanied by increased caspase-1 cleavage. Consistent with this, SDG-induced GSDMD-N-terminal fragment cleavage and pyroptosis were reduced by siRNA-mediated silencing of caspase-1 or treatment with the specific caspase-1 inhibitor VX-765 treatment, suggesting that active caspase-1 further induces pyroptosis. A mechanistic study showed that SDG induced reactive oxygen species (ROS) accumulation and inhibits phosphatidylinositol 3-kinase (PI3K) phosphorylation and increases pyroptosis, while increasing GSDMD and caspase-1 cleavage and enhancing expression of BCL2-associated X (BAX), which could be rescued by the ROS scavenger (NAC), suggesting that SDG-induced GSDME-dependent pyroptosis is related to the ROS/PI3K/AKT/BAX-mitochondrial apoptotic pathway. In vivo results showed that SDG significantly inhibited tumor growth and induced pyroptosis in the HCT116-CRC nude mouse model. In conclusion, our findings suggest that the anticancer activity of SDG in CRC is associated with the induction of GSDMD-dependent pyroptosis by SDG through the generation of ROS/P13K/AKT/BAK-mitochondrail apoptosis pathway, providing insights into SDG in its potential new application in cancer treatment.

KEYWORDS

caspase-1, GSDMD, pyroptosis, ROS, secoisolariciresinol diglucoside (SDG)

1 | INTRODUCTION

Colorectal cancer (CRC) is one of the most frequently encountered neoplasms in the world. The incidence and mortality rate of CRC are rising globally (Chen et al., 2016; Siegel et al., 2018). There is increasing evidence that most anticancer therapies trigger apoptosis-a type of programmed cell death (PCD) to eliminate tumor cells (Ouyang et al., 2012). Although chemotherapy is the main strategy for a variety of cancers, these strategies are greatly limited due to high recurrence rates, drug resistance, and strong side effects during treatment (Andersen et al., 2019). A major mechanism explaining the resistance of tumor cells to evade drug-induced apoptosis is the development and activation of antiapoptotic systems (Takagi et al., 2015). Therefore, a new drug capable of triggering nonapoptotic PCD is urgently needed.

Pyroptosis, a new type of PCD, also known as inflammatory necrosis, is a proinflammatory form of cell death (Jorgensen & Miao, 2015). Previous studies have provided evidence that, as a member of the gasdermin superfamily, gasdermin D (GSDMD) can induce apoptosis to pyroptosis upon caspase-1 cleavage (Ding et al., 2016; Shi et al., 2015). Activated caspases cleaves GSDMD in an interdomain linker to release the N-terminal domain and form membrane pores to cause pyroptosis, as evidenced by the cell membrane ballooning, the lactic dehydrogenase (LDH) activity elevation, and the increase of propidium iodide (PI) uptake (Xi et al., 2016). Recent studies have shown that chemotherapy drug-activated caspase-1 can also cleave GSDMD in the interdomain linker, releasing the N-terminal domain and forming membrane pores leading to pyroptosis, membrane ballooning, and elevated LDH activity, and increased PI uptake (Wang et al., 2019). Although there are many studies of GSDMD-dependent pyroptosis in tumor development, including CRC (Wu et al., 2020; Y. Zhang et al., 2021), the role of canonical or noncanonical pyroptosis in tumors is poorly clarified. Therefore, drugs that cause pyroptosis of cancer cells can well complement traditional PCD-based apoptotic anticancer drugs.

The secoisolariciresionol diglucoside (SDG) is a plant lignan isolated from flaxseed with anti-inflammatory (Rom et al., 2018) and antioxidative (Pilar et al., 2017) properties. SDG has been reported to inhibit various types of tumors (Tannous et al., 2020), including lung cancer, breast cancer, and so on (Bowers et al., 2019; Li et al., 1999). SDG triggers apoptosis in acute lymphoblastic leukemia cells through reactive oxygen species (ROS)-generated mitochondrial membrane potential (MMP) breakdown and DNA damage (Tannous et al., 2020). SDG inhibits the growth of CRC cell lines by downregulating G1-phase cyclins and CDKs, and upregulating p21WAF1/CIP1 (Chikara et al., 2017; Jenab & Thompson, 1996). These findings indicate that SDG has great potential as a pharmaceutical compound for the treatment of cancer. However, studies on its anticancer effects and underlying mechanisms in CRC have not been reported.

To explore how SDG induces pyroptosis in CRC cells and exerts its antitumor effect. In this study, we aimed to investigate the effects of SDG on CRC by activating the ROS/PI3K/AKT/BAX-mitochondrial apoptotic pathway in vitro and in vivo.

2 | MATERIALS AND METHODS

2.1 | Animals

All animal experiments were performed in accordance with protocols approved by the Institutional Animal Care and Use Committee. Male BALB/c nude mice (6 weeks) were purchased from Beijing Vital River Laboratory Animal Technology Co., Ltd. The experiment was approved by the Ethics Committee of General Hospital of Ningxia Medical University (2019-103).

2.2 | Cell lines and culture conditions

Human CRC cell lines (LOVO, SW620, SW480, HT29, and HCT116) were purchased from the American Type Culture Collection (ATCC). CRC cells were maintained in RPMI 1640 medium (Gibco) supplemented with 10% FBS (Thermo Fisher Scientific) and incubated at 5% CO_2 at 37°C.

2.3 | Chemicals and antibodies

SDG was purchased from MedChemExpress. *N*-Acetyl cysteine (NAC) was purchased from Abcam (Abcam), GSK'872 was purchased from Sigma-Aldrich, the caspase-1 specific inhibitor VX-765 and 740Y-P were purchased from MedChemExpress. Primary antibodies of caspase-1, caspase-4, caspase-5, caspase-11, GAPDH, and GSDMD were purchased from Abcam (Abcam). Antibodies against BCL2-associated X (BAX), cytochrome *c*, phosphorylated-PI3K (p-PI3K), phosphorylated-AKT (p-AKT), PI3K, and AKT were purchased from Cell Signaling Technology.

2.4 | Cell viability assay (CCK-8)

Exponentially growing HCT116 cells were seeded into 96-well culture plates (6000 cells/well) for 24 h before stimulation. Cells were treated with different doses of SDG or NAC for the indicated times. Cell viability was determined by CCK-8 (cell counting kit-8 assay, Dojindo Laboratories) assay according to the manufacturer's protocol. Half maximal inhibitory concentration (IC_{50}) was calculated from cell viability values using Prism 8 software (GraphPad). In other experiments, HCT116 cells were pretreated with caspase 4 inhibitor (Z-YVAD-FMK) for 3 h and subjected to CCK-8 assay.

2.5 | LDH release assay

Briefly, cell culture supernatants were collected after various treatments and assayed for LDH activity using an LDH-release kit (Promega) according to the manufacturer's instructions. The absorbance was measured at 450 nm.

2.6 | siRNA knockdown

HCT116 cells were seeded in six-well plates. After 24 h, SiRNA transfections were performed using transfection reagent according to the manufacturer's instructions with caspase-1/4/5/11-specific siRNA duplexes (siRNA-caspase-1/4/5/11) under the same conditions transfected cells, GSDMD- and BAX-specific siRNA duplexes (siRNA-GSDMD), or control siRNA (NC) duplexes. All siRNA duplexes were purchased from Genepharma. After 72 h, transfected HCT116 cells were treated with SDG (50 μmol/L) at the indicated concentrations and subjected to subsequent analyses.

2.7 | Microscopy imaging

To examine the morphology and death process of pyroptotic cells, cells were seeded in six-well plates and treated with SDG at the indicated concentrations. After processing, bright-field images of cells were captured using an Olympus IX53 microscope.

2.8 | Measurement of MMP

MMPs in HCT116 cells were measured using the fluorescent dye JC-1 (Thermo Fisher Scientific Co., Ltd.) according to the manufacturer's instructions. After culturing in 24-well plates, HCT116 cells were treated with SDG at the indicated concentrations (0, 5, 25, 50 μmol/L) and then incubated with fluorescent dye JC-1 staining solution for 20 min at 37°C. Cell images was monitored using an Olympus IX53 microscope.

2.9 | Lytic cell death assay

Briefly, HCT116 cells were seeded in six-well plates and treated with indicated concentrations of SDG. After treatment, cells were stained with Hoechst33342 solution to reveal cell nuclei and PI solution to indicate necrotic cells according to the manufacturer's instructions. The bright-field cell images were captured using the fluorescence microscope.

2.10 | Measurement of ROS

The ROS levels were measured using H2DCF-DA fluorescence probe as previously described. Briefly, after SDG or NAC treatment, treated-cells (HCT116) were collected, washed twice with phosphate-buffered saline (PBS), and stained with H2DCF-DA (5 μmol/L) for 30 min at 37°C in the dark. Subsequently, the level of ROS was analyzed with flow cytometer (BD).

2.11 | Flow cytometry analysis

Briefly, HCT116 cells were treated with SDG at the indicated concentrations. Cells were collected, washed twice with PBS, and stained using the Annexin V-FITC/PI Apoptosis assay kit by following the manufacturer's instructions. Flow cytometry analysis was performed using a BeckMan CytoFlex (BeckMan).

2.12 | Western blot analysis

Cells or tumor tissues were washed twice with cold PBS and prepared in RIPA buffer (Beyotime Institute of Biotechnology) to collect proteins from cells or tumors. Protein concentration was measured using a BCA protein assay kit (Keygen biotech). Equal amounts of the protein samples (50 μg) were separated by 10% sodium dodecyl sulfate polyacrylamide gel electrophoresis, transferred to a polyvinylidene fluoride membrane (Hercules), and then detected with appropriate primary and secondary antibodies. Detection was performed using the ECL system (Advansta). Expression levels of proteins were normalized to total GAPDH.

2.13 | Animal study

Tumor cells (3×10^6) were suspended in 200 μl of serum-free-RPMI-1640/Matrigel mixture (3:1 volume) and injected subcutaneously into the back of BALB/c nude mice. Experiment (Kezimana et al., 2018) was performed as previously described and mice were treated with SDG (50, 150, and 200 mg/kg) once daily, respectively. After 24 days, the mice were euthanized, and the tumors were excised. Mice were monitored every 3 days for tumor volume ($[V = (L \times S2)/2]$) and body weight. Results were plotted as relative tumor volume and body weight fofrom the first day of treatment until the last day. The tumor tissues were fixed with formalin and subsequently embedded in paraffin. The sections of tumor tissues were iImmunohistochemistry (IHC) stained with the cell proliferation marker Ki67 (1:300).

2.14 | Statistical analysis

Statistical difference between groups were analyzed by using one-way analysis of variance or comparisons between two groups were tested for significance using the two-tailed Student's *t*-test. All data expressed as mean ± *SD* were analyzed using SPSS 22 software. $p < 0.05$ was considered statistically significant.

3 | RESULTS

3.1 | SDG induces distinct patterns of apoptosis and lytic cell death in HCT116 cells

The anticancer properties of SDGs in CRC cell lines were investigated, and cell viability was then assessed using the CCK-8 assay. As shown in Figure 1a, our results showed that SDG treatment dose-dependently inhibited CRC cell viability compared with control. In the meantime, we measured their half maximal inhibitory concentrations values with IC50 of 24.5 μmol (Table 1). Furthermore, our further study showed that SDG treatment significantly inhibited the cell viability of HCT116 cells in a time-dependent manner (Figure 1b). Consequently, our results suggest that SDG inhibits the viability of CRC cells in.

TABLE 1 IC_{50} of SDG in HCT116 cells.

Cell line	IC_{50} (μmol/L)[a]	*SD*(%)
HCT116	24.5	27.37

Abbreviation: SDG, secoisolariciresinol diglucoside.

[a]IC_{50} values represent as mean of three determinations.

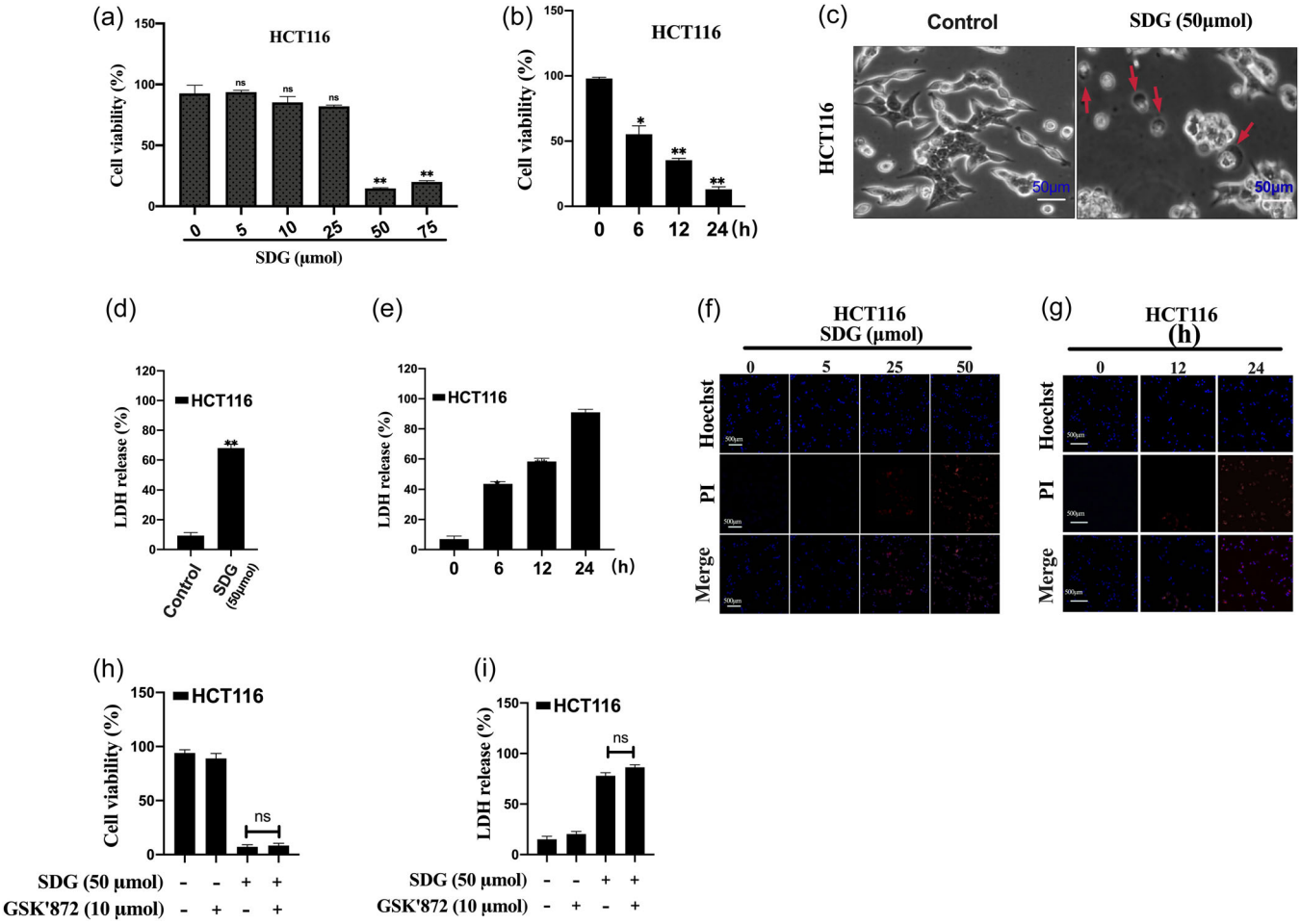

FIGURE 1 Secoisolariciresinol diglucoside (SDG) induces distinct patterns of apoptosis and lytic cell death in HCT116 cells. HCT116 (a) cells were treated with SDG (0, 5, 10, 25, 50, 75 μmol) at indicated time. Treated the HCT116 (b) cells with 50 μmol/L of SDG for 24 h. HCT116 cells viability was analyzed by CCK-8 assay. (c) HCT116 cells were treated with SDG (24 h). Red arrowheads indicate the large bubbles (termed pyroptotic bodies) emerging from the plasma membrane, and the images of HCT116 cells observed by microscopy. Scale bar = 50 μm. (d) HCT116 cells were treated with SDG at indicated graded concentrations for 24 h. The release of lactic dehydrogenase (LDH) from SDG-treated HCT116 cells was measured by ELISA Kit. (e) LDH secretion was measured by ELISA Kit in HCT116 cell lines treated with SDG (50 μmol/L) at different points in time (0, 6, 12, and 24 h). (f) HCT116 cells were treated with SDG at the indicated concentration for 24 h. The percentage of propidium iodide (PI) (red) positive cells were observed by fluorescent microscopy. Scale bar = 500 μm. (g) The fluorescent images of HCT116 cells stained with PI and Hoechst 33342 were taken at the indicated timepoints after treatment with SDG (50 μmol/L). Scale bar = 500 μm. (h,i) At the indicated timepoints, the percentage of LDH release in the culture supernatants from HCT116 was measured after treatment with SDG or GSK'872. HCT116 cells viability was analyzed by CCK-8 assay. Error bars in this and subsequent figures: mean ± *SD* of three independent experiments. NS, no significance; SD, standard deviation; $^{*}p < .05$; $^{**}p < .01$ versus SDG alone.

Next, we examined the pyroptotic cell death effect of SDG in HCT116 cells. To reveal the type of cell death induced by SDG, the Olympus IX53 microscope imaging system was used to observe the cell morphological changes and cell death process of HCT116 cells. Morphologically, as shown in Figure 1c, a total of 50 μmol of SDG-induced HCT116 cells gradually shrank, followed by the swell and rupture of the cell membrane, and eventually cell death, which is very similar to the pyroptosis induced by the N-terminus of GSDMD (Shi et al., 2015). Furthermore, after HCT116 cells were exposed to SDG. There was increasing release of LDH (LDH, an indication of pyroptotic cell cytotoxicity) in dose- and time-dependent manners, further indicating plasma membrane rupture and leakage (Figure 1d,e). In addition, the Hoechst33324/PI staining (PI could penetrate into the dying cells with the loss of cell membrane integrity) results demonstrated that SDG treatment increased the percentage of PI-positive cells for HCT116 in dose- and time-dependent manners (Figure 1f,g). These imaging results clearly indicate that SDG can change the plasma membrane permeability in CRC cells, and ultimately lead to lytic cell death. Cell undergoing necroptosis also showed cell swelling, membrane disruption, and pyroptotic lysis. Moreover, to reveal the type of cell death induced by SDG, we also used the necroptosis inhibitor GSK'872 to distinguish pyroptosis from necroptosis (Wallach et al., 2016). As expected, GSK'872 had no significant effects on SDG-induced cell death and LDH release compared to the control group (Figure 1h,i). These data indicated that SDG-induced CRC cells undergo a transition from apoptosis-to-pyroptosis and ultimately lead to lytic cell death.

3.2 | Cleavage of GSDMD is involved in SDG-induced pyroptosis in CRC cells

Because GSDMD has been reported to act as pyroptotic executioners (Shi et al., 2015), we investigated whether SDG-induced pyroptotic death in HCT116 cells is associated with cleavage of GSDMD. In this study, we employed western blot analysis to detect the activated GSDMD. As shown in Figure 2a, we found that GSDMD was highly expressed in the HCT116 cell lines. As anticipated, SDG treatment significantly increased the level of activated GSDMD (Figure 2b), a marker of pyroptosis, in HCT116 cells in a dose-dependent manner. In the meantime, siRNAs was used to silence the expression of GSDMD in HCT116 cell lines (Figure 2c). Then, western blot analysis confirmed that the N-terminal fragment of GSDMD was barely detected in GSDMD-knockdown cells treated with SDG (Figure 2d). Moreover, the flow cytometry analysis result showed that siRNA knockdown of GSDMD expression significantly decreased the percentage of pyroptotic cells in Annexin V-FITC/PI-stained HCT116 cells (Figure 2e). In addition, as shown in Figure 2f–h, siRNA inhibiting GSDMD expression did decrease SDG-induced plasma membrane ballooning and LDH release, but did not ultimately rescue cell death in response to SDG treatment. Taken together, all these results suggested that GSDMD is a key effector of SDG-induced pyroptosis in CRC cells.

In this case, we also wondered whether this SDG-induced pyroptosis was a general phenomenon. Interestingly, upon SDG stimulation, we found that the expression level of GSDMD was significantly upregulated in HCT116 cells compared to other CRC cell lines, and this SDG-induced pyroptosis appeared to be specific for HCT116 cells (Figure 2i).

3.3 | GSDMD was cleaved in SDG-induced noncanonical pyroptosis by caspase-1

Emerging evidence indicates that cell pyroptotic death was shown to be triggered by the N-terminal domain of GSDMD due to cleavage by the different inflammatory caspases (caspase-1/4/5/11 in humans) (Shi et al., 2015). Subsequent western blot analysis analyses, the results showed that SDG significantly increased the level of activated caspase-1 in HCT116 cells (Figure 3a), but we did not find the activation of caspase-4/5/11 in HCT116, indicating that GSDMD may be cleaved by the active caspase-1. To confirm the involvement of caspase-1 in SDG-triggered pyroptotic death, we knocked down the expression of caspase-1 in HCT116 cells using siRNA (Figure 3b). Notably, we found that knockdown of caspase-1 inhibited the generation of the N-terminal GSDMD (Figure 3c). Furthermore, SDG-induced LDH release and cell death were remarkably attenuated in HCT116 cells in the presence of caspase-1 knockdown (Figure 3d,e). Furthermore, HCT116 and SW620 cells were pretreated with the caspase-1-specific inhibitor VX-765 and then treated with SDG. We found that VX-765 treatment inhibited the release of LDH (Figure 3f) and the cleavage of GSDMD (Figure 3g) triggered by SDG. Thus, these data suggest that SDG induces noncanonical pyroptotic death by activating caspase-1 in HCT116 cells.

3.4 | SDG activated the BAX-mitochondrial intrinsic apoptotic pathway to elicit GSDMD-dependent pyroptosis

Recent findings have reported that GSDMD-mediated pyroptosis can be triggered by the BAX-mitochondrial intrinsic apoptotic pathway (Wei et al., 2020). Exposure of HCT116 cells to SDG caused disruption of MMP, as evidenced by an increase in the proportion of cells with green fluorescence and a decrease in the proportion of cells with red JC-1 fluorescence (Figure 4a). Furthermore, we also examined the level of BAX and cytochrome *c* in response to SDG by western blot analysis. As expected, SDG effectively increased the protein levels of BAX and cytochrome *c* (Cyto *c*) in dose-dependent manners, indicating that the SDG-induced pyroptosis in HCT116 cells might be mediated through BAX-mitochondrial intrinsic apoptotic pathway (Figure 4b). Additionally, the siRNA technology was used to verify whether BAX is involved in pyroptosis induction. In HCT116 cells, knockdown of BAX resulted in the visible decrease of N-GSDMD generation, cleaved caspase-1, Cyto *c* (Figure 4c) and LDH release (Figure 4d). These results demonstrated that SDG

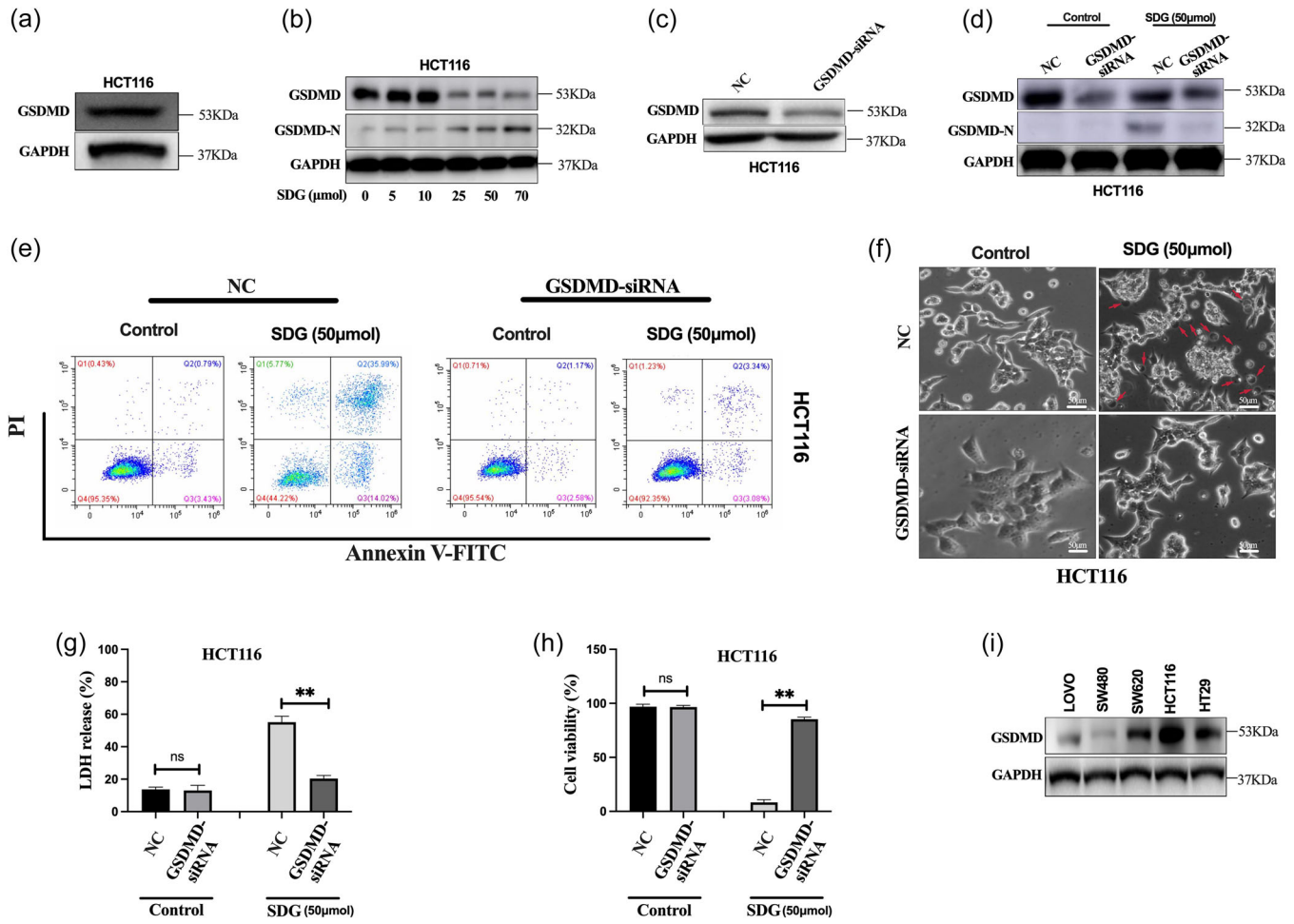

FIGURE 2 Cleavage of GSDMD is involved in secoisolariciresinol diglucoside (SDG)-induced pyroptosis in colorectal cancer (CRC) cells. (a) Gel images of GSDMD expression levels in HCT116 cells. (b) Cleavage of GSDMD were monitored by immunoblot analysis 24 h after stimulation of HCT116 cells with SDG (0–70 μmol/L). (c) HCT116 cells were transfected with GSDMD-siRNA (siRNA knockdown of GSDMD) or control NC (siRNA, negative control) for 24 h, then the GSDMD, GSDMD-N, and GAPDH expression was detected by western blot analysis. (d) Control siRNA (NC) and GSDMD-siRNA HCT116 cells were treated with SDG (50 μmol/L) for 24 h, cell protein was then harvested for detecting GSDMD, GSDMD-N, and GAPDH by western blot. (e) NC and GSDMD-siRNA CRC cells were treated with SDG (50 μmol/L), stained by Annexin V-FITC and propidium iodide, and was detected by flow cytometry. (f) The pyroptotic features of HCT-116 cells treated with SDG in the presence or absence of GSDMD-siRNA transfection, scale bar = 50 μm. (g) and (h) HCT116 cells were transfected with GSDMD-siRNA (siRNA knockdown of GSDMD) or control NC (siRNA, negative control) and then treated with SDG (50 μmol/L) at 24 h after transfection, cell viability was measured by CCK-8 assay, and lactic dehydrogenase (LDH) secretion were measured using ELISA Kit. (i) Immunoblots were performed to detect pyroptosis-related proteins in CRC cells (LOVO, SW480, SW620, HCT116, and HT29) extracts. GAPDH was used to determine the amount of loading proteins. All the data are presented as the mean ± *SD* from three independent experiments. $^{*}p < .05$, $^{**}p < .01$ compared with control group. SD, standard deviation.

induces GSDMD-dependent pyroptosis in CRC cells by activating the BAX-mitochondrial pathway.

3.5 | SDG-induced noncanonical pyroptotic requires PI3K/AKT signaling pathway

Previous reports have confirmed that the PI3K/AKT signaling pathway is involved in the progression of CRC, and the activation of PI3K/AKT signaling promotes pyroptosis (Pei et al., 2019). To further elucidate the cellular mechanism of pyroptosis inhibition by SDG, we analyzed whether the PI3K/AKT signaling pathway affects SDG-induced pyroptosis. Our study found that SDG stimulation markedly decreased the phosphorylation levels of PI3K and AKT in HCT116 cells compared to the control group (Figure 5a). Notably, we found that the PI3K activator 740Y-P (Cayman) effectively reduced the release of LDH and inhibited the cleavage of GSDMD, and the protein level of caspase-1 was significantly reduced (Figure 5b,c). As we expected, 740Y-P significantly decreased SDG-induced BAX protein expression (Figure 5c). Consequently, BAX is a downstream factor of PI3K/AKT. Thus, these data indicate that PI3K/AKT signaling pathway is

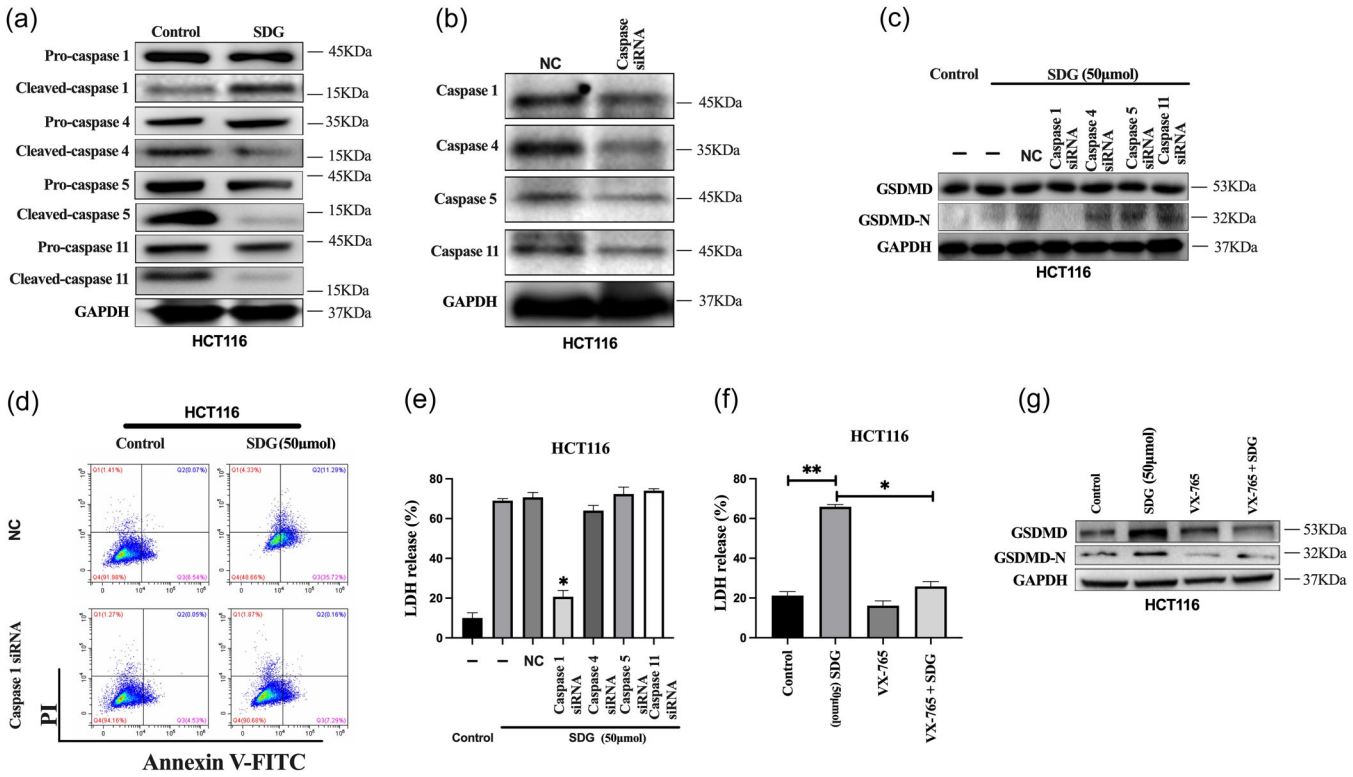

FIGURE 3 GSDMD was cleaved in secoisolariciresinol diglucoside (SDG)-induced pyroptosis by caspase-1. (a) HCT116 were treated with SDG for 24 h, total cellular extracts were prepared, cell protein was then harvested for detecting caspase-1/-4/-5/-11, and GAPDH by western blot. (b) The cells were then incubated with 50 μM SDG reagent for 24 h, HCT116 cells were transfected with siRNA targeting caspase-1/-4/-5/-11 or control siRNA. Cell proteins were subjected to western blot analysis analyses using antibodies against caspase-1/-4/-5/-11, and GAPDH. (c) After HCT116 cells were treated with caspase-1/-4/-5/-11 knockdown in the absence or presence of SDG (50 μmol/L) for 24 h, GSDMD-N terminus were detected by western blot in cell protein. (d) Annexin V-FITC and propidium iodide (PI) stained HCT116 cells were analyzed by Annexin V-FITC/PI apoptotic detecting kit. (e) The release of lactic dehydrogenase (LDH) in HCT116 cells was measured by ELISA Kit after transfection with siRNA. (f) The release of LDH in HCT116 cells was measured by LDH assay kit. (g) Western blot analysis of GSDMD and GSDMD-N protein levels. GAPDH was used to determine the amount of loading proteins. All the data are presented as the mean ± *SD* from three independent experiments. $^{*}p < .05$, $^{**}p < .01$ compared with control group. SD, standard deviation.

involved in SDG-mediated pyroptosis by cleaved of GSDMD via caspase-1 activation.

3.6 | SDG induces pyroptotic cell death via the ROS/PI3K/AKT pathway in HCT116 cells

SDG has been found to induce tumor cells apoptosis by activating the ROS-dependent mitochondrial intrinsic apoptotic pathway (Tannous et al., 2020). Because ROS have been reported to act as pyroptotic executioners. Thus, we investigated whether ROS are involved in SDG-induced CRC cells pyroptosis. Here, our study found that SDG treatment significantly increased the intracellular ROS level in HCT116 cells. Furthermore, NAC (NAC, an inhibitor of ROS) could remarkably decrease the ROS level in SDG-treated HCT116 cells as assessed by Flow cytometric (Figure 6a). To further determine the role of intracellular ROS accumulation in SDG-induced pyroptosis, CRC cells (HCT116) were stimulated with SDG in the presence of NAC and the cell viability (Figure 6b) and LDH release (Figure 6c) were assessed. As expected, the NAC can rescue SDG-induced cell death and LDH release compared to the control group. In addition, SDG treatment upregulated the protein levels of cleavage of caspase-1, and GSDMD, which can be significantly reversed by ROS inhibitor NAC (Figure 6d). Numerous reports have demonstrated that ROS signaling pathway is the upstream signal transducers that activates the PI3K/AKT-mediated cascades (Zhao et al., 2017). To investigate whether the increased ROS level are involved in the activation of PI3K/AKT in SDG-treated HCT116 cells, the protein expression of AKT in SDG or SDG plus NAC treated HCT116 cells was detected by using western blot. In HCT116 cells, SDG significantly downregulated the protein levels of AKT and upregulated the protein levels of BAX, while combined treatment with NAC can reverse these changes (Figure 6e). Taken together, these results revealed that SDG plays an important role in SDG-induced pyroptosis by inhibiting the PI3K/AKT signaling pathway by increasing intracellular ROS levels in HCT116 cells.

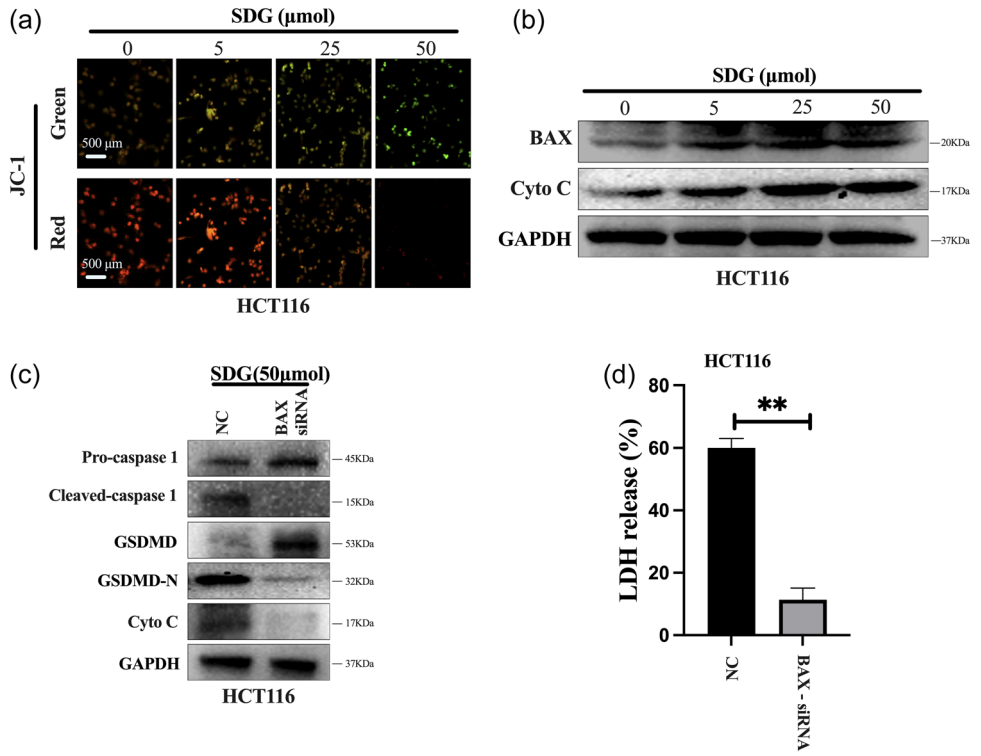

FIGURE 4 Secoisolariciresinol diglucoside (SDG) activated the BAX-mitochondrial intrinsic apoptotic pathway to elicit GSDMD-dependent pyroptosis. HCT116 cells were treated with SDG for 24 h. (a) The MMP was measured by fluorescent microscope, scale bar = 500 μm. (b)Total cellular extracts were prepared and subjected to western blot analysis analyses using antibodies against BAX and Cyto *c*. (c) Gel images of GSDMD-N, Cyto *c*, and cleaved caspase-1 expression levels in HCT116 cells in the presence or absence of BAX knockdown. (d) Lactic dehydrogenase (LDH) release were measured by LDH assay in HCT116 cells in the presence or absence of BAX knockdown. Protein levels are expressed as mean ± *SD* (*n* = 3). $^{**}p < .01$ versus control. SD, standard deviation.

3.7 | SDG inhibited the tumor formation and induced colon cancer cells pyroptosis in vivo

To further investigate the effect of SDG in inhibiting tumor formation and inducing pyroptosis in colon cancer, HCT116 cells and their control cells were subcutaneously injected into the back of BALB/c nude mice. Four diets were compared: a basal diet (control group) and the basal diet supplemented with 50, 150 or 200 mg/kg of SDG. The experimental results of nude mice showed that SDG significantly reduced tumor volume and tumor weight (Figure 7a–c) in HCT116 tumor-bearing mice as compared with the control. Because tumor growth is the result of tumor cell proliferation and apoptosis. The subsequent IHC analysis of HCT116 (Figure 7d,e) proliferation marker Ki67, further revealed a smaller number of Ki67positive cells was observed in tumor mass generated from treatment with SDG compared to those of control group. Moreover, we explored whether reductions in tumor volume and tumor weight were associated with SDG-induced pyroptosis. The level of serum LDH is increased in either SDG treatment group as compared with control group (Figure 7f). Additionally, western blot analysis analyses showed that SDG treatment upregulated the expression of N-GSDMD and cleaved-caspase-1 in a dose-dependent manner (Figure 7g). Collectively, these results showed that SDG might inhibit the growth of CRC tumors in vivo by inducing pyroptosis (Figure 8).

4 | DISCUSSION

CRC has been identified as the second leading cause of neoplasms death worldwide with incidence estimation of 16.5 million (Global Burden of Disease Cancer Collabroation et al., 2017; Sieminska & Baran, 2020). Several studies reported that chemotherapy is an important part of the comprehensive treatment for advanced CRC, but it only provides limited survival benefit for patients (Amable, 2016; Mármol et al., 2017; McQuade et al., 2017). Therefore, it is urgent to find more accurate drugs with high curative value and low toxicity for the treatment of CRC. However, the research on pyroptosis and related drugs in the treatment of CRC is still limited. In this study, cell viability assay revealed that SDG could inhibit the growth of HCT116 cells. Additionally, an in vivo experimental CRC model demonstrated that treatment with SDG significantly inhibited the CRC tumor growth. Our data strongly demonstrate the great potential of SDG as a new cancer therapy.

Numerous research reports have confirmed that apoptosis is genreally considered to be the main form of cell death that leads to

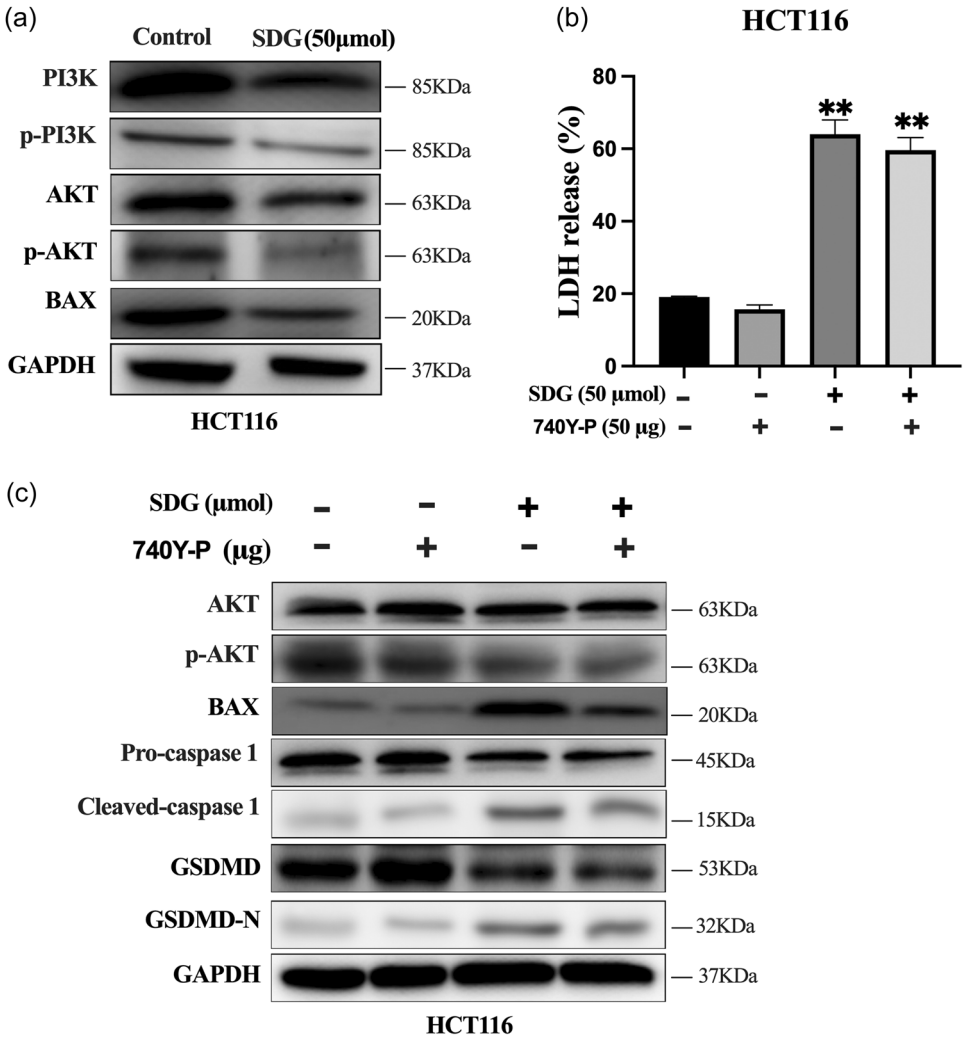

FIGURE 5 Secoisolariciresinol diglucoside (SDG)-induced pyroptotic requires PI3K/AKT signaling pathway. (a) HCT116 cells were treated with SDG (50 μmol/L) for 24 h, cell protein was then harvested to detect PI3K, p-PI3K, AKT, p-AKT, BAX, and GAPDH by western blot. (b) HCT116 cells were treated with SDG or cotreated with 740Y-P (50 μg/ml) and SDG (50 μmol/L), as indicated by the concentration shown, for 24 h. After treatment, the release of lactic dehydrogenase (LDH) from HCT116 cells was measured by ELISA Kit. (c) HCT116 cells were pretreated with SDG (50 μmol/L) in the absence or presence of 740Y-P (50 μg/ml) for 24 h. After treatment, cell protein was then harvested to detect the expression of AKT, p-AKT, BAX, cleavage of GSDMD, and caspase-1 by western blot. All the data are presented as the mean ± *SD* from three independent experiments. $^{*}p < .05$, $^{**}p < .01$ versus control using one-way analysis of variance. SD, standard deviation.

the regulation of tumor therapies (Hou et al., 2020; Tsuchiya, 2021; Woo et al., 2020). The use of SDG in cancer therapy has been attributed to its ability to inhibit cancer cell growth and induce cancer cell apoptosis (Bowers et al., 2019; Li et al., 1999; Tannous et al., 2020). Recent findings have reported the apoptotic induction activity of SDG in CRC (Danbara et al., 2005). In the present study, we extend the conventional view and identify the involvement of GSDMD-dependent pyroptosis in the treatment of SDGs in CRC, supported by the following evidence. Firstly, our results showed that the hallmark features of pyroptosis, such as GSDMD cleavage, balloon-like bubbles, LDH release, and PI-positive staining, were observed in SDG-treated CRC cells. It should be noted that cells undergoing necroptosis also exhibit plasma membrane permeabilization, cell swelling, and lysis (Lu et al., 2018). Remarkably, GSK'872, an inhibitor of necroptosis, had no significant effects on cell viability and LDH release. The results clearly indicate that cell death triggered by SDG in our study was not necroptosis. Secondly, we compared the GSDMD protein expression in HCT116 cell lines, and confirmed that GSDMD was commonly expressed in CRC cell lines. In addition, during pyroptosis, pores open in the cell membrane, allowing Annexin V to enter the cells and stain the inner leaflets of the membrane. In contrast, membrane impermeant dyes, such as PI (Fink & Cookson, 2006), stain pyroptotic cells by entering through the pores, but do not stain apoptotic cells (Miao et al., 2011; Silveira & Zamboni, 2010). We found that SDG-treated HCT116 cells proceeded directly to the Annexin V and PI double-positive stage, while knockdown of GSDMD delayed the process with increasing the proportion of Annexin V single-positive cells and decreasing the percentage of double-positive

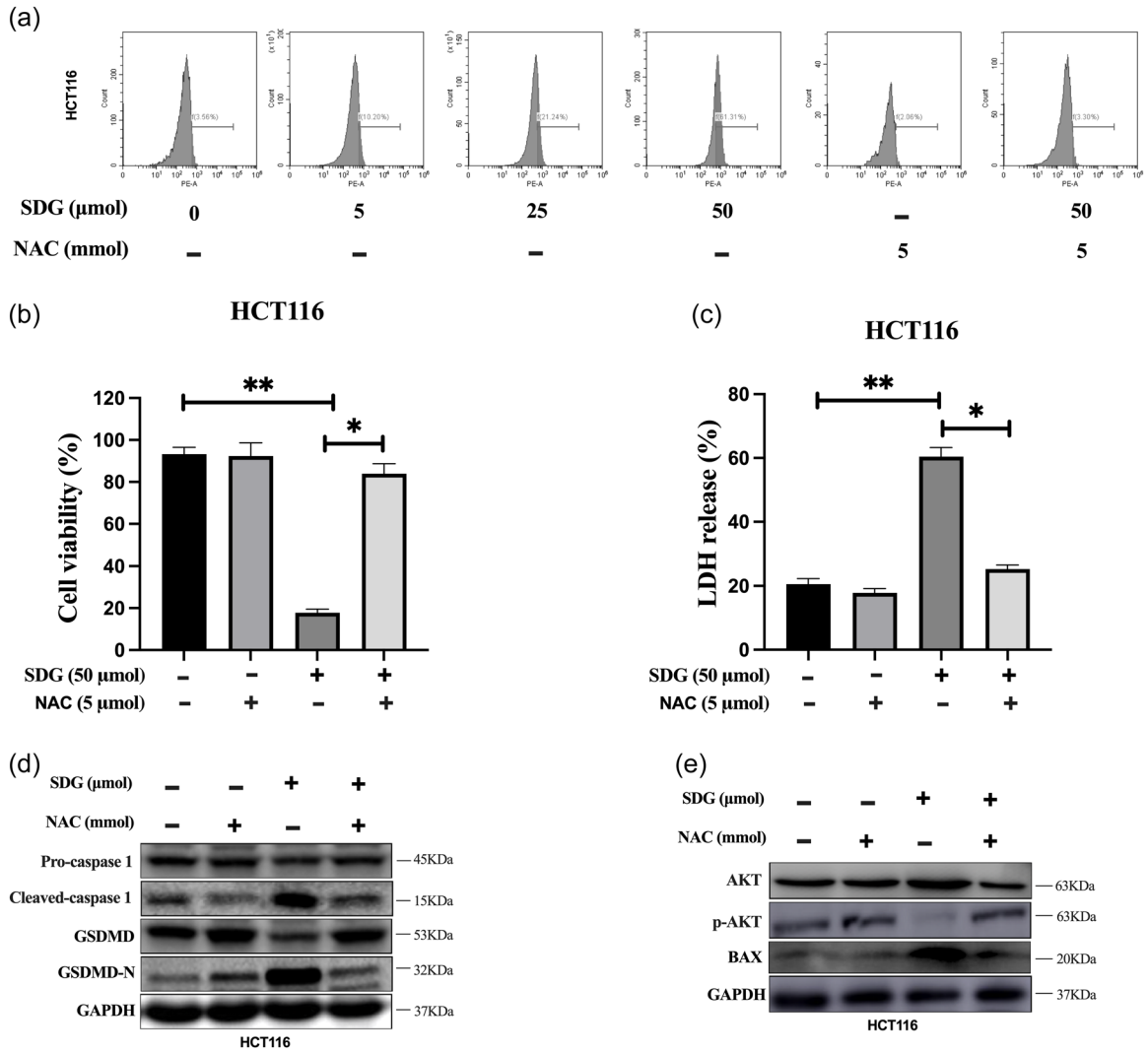

FIGURE 6 Secoisolariciresinol diglucoside (SDG) induces pyroptotic cell death via the ROS/PI3K/AKT pathway in HCT116 cells. (a) HCT116 cells treated with SDG in the presence or absence of NAC, intracellular ROS content was measured with flow cytometry. (b) and (c) HCT116 cells treated with SDG in the presence or absence of NAC, cell viability and lactic dehydrogenase (LDH) release were measured. (d) and (e) HCT116 cells treated with SDG in the presence or absence of NAC, after treatment, cell protein was then harvested to detect BAX, cleaved caspase-1, cleaved GSDMD, PI3K/AKT, and GAPDH by western blot. All the data are presented as the mean ± *SD* from three independent experiments. $^{*}p < .05$, $^{**}p < .01$ versus control. SD, standard deviation.

cells. GSDMD knockdown did not rescue cell death in response to SDG treatment, whereas resulted in reduction of SDG-induced LDH release and plasma membrane ballooning, further confirming from pyroptosis to apoptosis.

Studies have confirmed that different inflammatory caspases can activate two modes of cell pyrolysis, promptly either canonical or noncanonical pyroptosis (Bergsbaken et al., 2009). In humans, pyroptosis is mediated by inflammatory caspases (caspase-1, caspase-4, and caspase-5), which may be activated by inflammasomes (Martinon & Tschopp, 2007). The inflammasome pathways include the caspase-1-dependent canonical pathway and caspase-1-independent noncanonical pathway. Among them, caspase-1, also known as IL-1β-converting enzyme, leads to pore formation in the cell membrane and the maturation and release of IL-1β and IL-18 cytokines, thereby induce pyroptosis (Martinon & Tschopp, 2005). Caspase-1 dimerization and self-activation are induced by inflammasomes, which are composed of a PRR, the adaptor ASC, and pro-caspase-1 (Martinon & Tschopp, 2007). The noncanonical pathway in humans involves the activation of caspase-1 (Martinon & Tschopp, 2007). Caspase-1 cleaves GSDMD, thereby triggering pyroptosis. In human macrophages, caspase-1 activation by *Legionella pneumophila* induced cell death and IL-1α secretion (Casson et al., 2015). Intracellular lipopolysaccharide (LPS) directly interacts with caspase-1 and induces cell pyroptosis (Viganò et al., 2015). In this study, we found that the expression of caspase-1 was significantly high during SDG-induced pyroptosis of HCT116 cells. However, SDG treatment did not considerably change caspase-1 expression at protein levels and did not change the amount of cleaved caspase-1. Notably, we

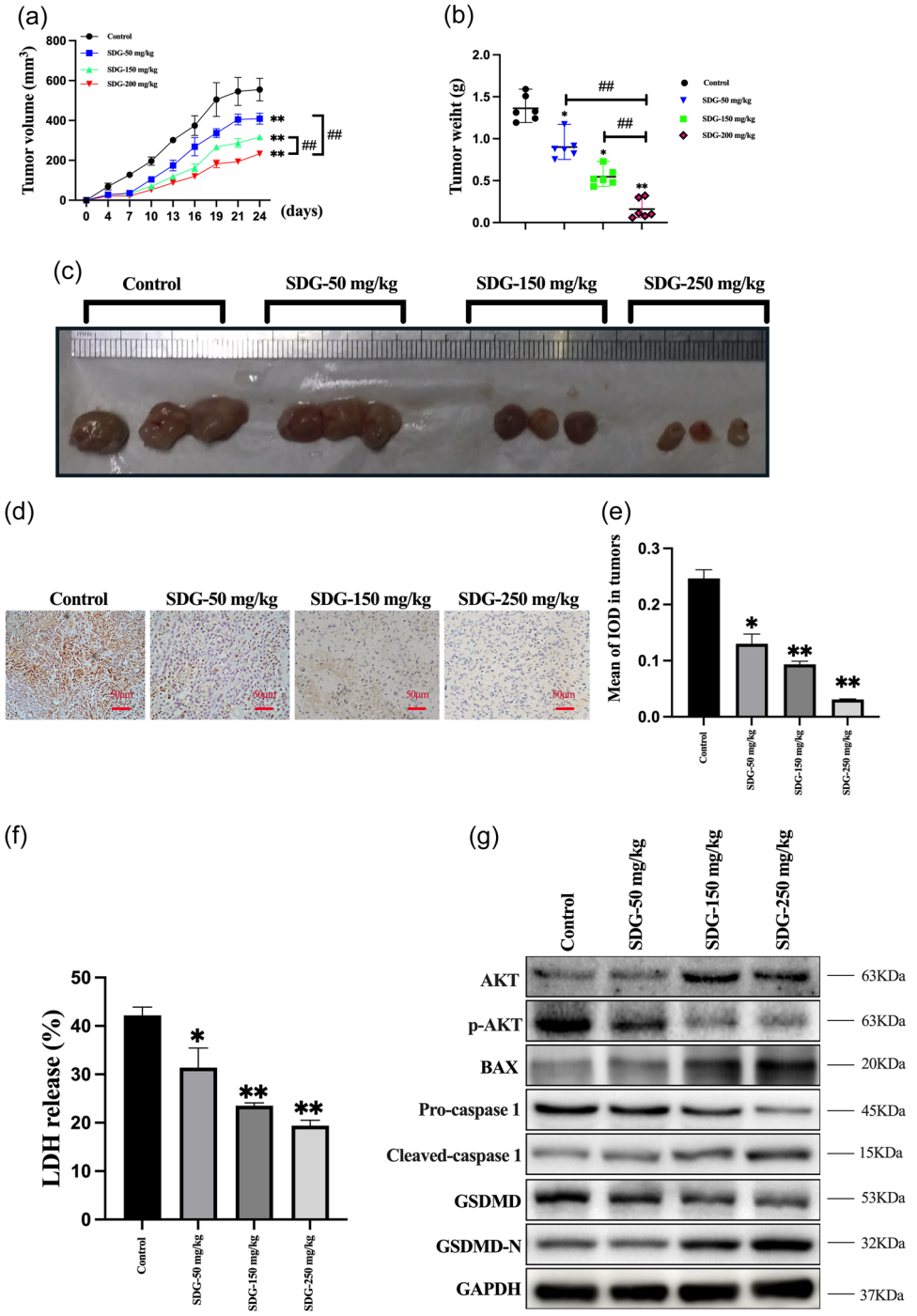

FIGURE 7 Secoisolariciresinol diglucoside (SDG) inhibited the tumor formation and induced colon cancer cells pyroptosis in vivo. The effect of SDG treatment on tumor volume (a–c) and tumor weight (c–f) at 0–24 days in HCT116 tumor-bearing mice. (d,e), representative images of Ki67 expression in the tumor tissues by immunohistochemistry and its relevant quantification of the numbers of positive cell, scale bar = 500 μm. (f,g) After treatment, gel images of PI3K, AKT, BAX, and cleaved caspase-1, GSDMD-N expression levels. Scale bar = 100 μm. $^{*}p < .05$, $^{**}p < .01$ versus vehicle treatment; $^{\#}p < .05$, $^{\#\#}p < .01$ versus indicated treatment.ent experiments. $^{*}p < .05$ versus control using one-way analysis of variance.

found that knockdown of caspase-1 suppressed the generation of the N-terminal GSDMD and release of LDH in HCT116. Therefore, these data indicate that SDG induces noncanonical pyroptosis by activating caspase-1.

In addition, the preliminary observation of signaling interrelation between pyroptosis and apoptosis suggest that the two death modes may reciprocally regulate each other to produce cytotoxic inhibition (Fang et al., 2020) demonstrated that two forms of regulated cell

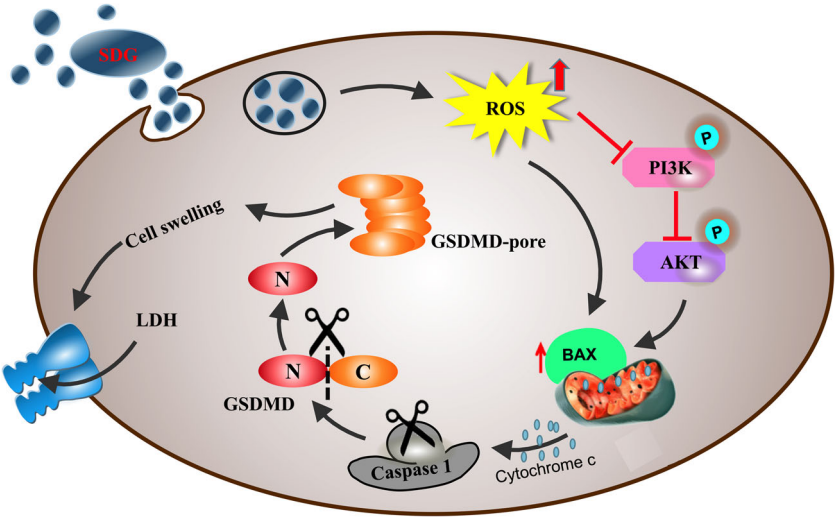

FIGURE 8 Abstract graphic. A schematic diagram of the molecular mechanism by which secoisolariciresinol diglucoside (SDG) induced noncanonical pyroptosis via the activation of the ROS/PI3K/AKT/BAX/Caspase-1/GSDMD signal axis in CRC cells. LDH, lactic dehydrogenase; ROS, reactive oxygen species.

death may exist simultaneously upon chemotherapy drugs exposure. Consistent with this previous study, our results indicated that the biochemical markers for apoptosis and pyroptosis were invariably synchronously detected in SDG-stimulated CRC cells. Knockdown of GSDMD switched SDG-induced cell death from pyroptosis to apoptosis, reinforcing the idea that therapy-induced pyroptosis may precede apoptosis. Furthermore, GSDMD has been reported to augment caspases activation and apoptotic cell death by targeting the ROS (Heilig et al., 2020). Cleavage of GSDMD by death receptor signaling bridges the extrinsic to the intrinsic apoptotic pathway (Fang et al., 2020; Feng et al., 2018). In conclusion, considering these results, we proposed that the signaling crosstalk between pyroptosis and apoptosis may have implications for determining the type of cell death. The GSDMD-dependent pyroptotic cell death can be triggered by the ROS signaling (Gao et al., 2018; Zheng & Li, 2020). Notably, our findings showed that SDG induced oxidative stress and increased the protein levels of BAX, cleaved-caspase-1, and N-GSDMD in HCT116 cells. In contrast, the siRNA of caspase-1 and the caspase-1-specific inhibitor VX-765 inhibited SDG-induced pyroptosis, suggesting that the activation of ROS-mediated caspases was required for SDG-induced pyroptosis in CRC cells. Lastly, mechanistic experiments in nude mice further demonstrated that SDG induced tumor cell pyroptosis in CRC tumors.

Many cellular processes in cancer are attributed to kinase signaling networks. PI3K/AKT signaling pathway plays a major role in regulating cancer cell pro-proliferative, antiapoptotic pathways, and differentiation. The over activation of these pathways is frequently observed in CRC, constituting a relevant target in cancer therapy (Brown & Banerji, 2017; Song et al., 2019). The upregulation of the PI3K/AKT signaling pathway is common in human cancers, including CRC, therefore, targeting AKT could provide an important approach for cancer prevention and treatment (Brown & Banerji, 2017; Yao et al., 2020). However, whether PI3K/AKT signaling pathway is involved in the SDG-induced pyroptosis remains unclear. In this present study, we found that SDG treatment significantly inhibited the phosphorylation of PI3K and AKT in HCT116 cells. Moreover, PI3K activator, 740Y-P inhibited the SDG-induced pyroptosis in HCT116 cells, as indicated by the LDH assay. These results suggest that, at least partially, PI3K/AKT signaling is involved in the SDG-induced pyroptosis. As we all know, PI3K/AKT pathway is associated with an intrinsic apoptotic pathway characterized by upexpression of BAX, release of cytochrome *c* from mitochondria and activation of caspase-1 (J. Zhang et al., 2016). Indeed, in our study, inhibited PI3K/AKT signaling pathway increased activation of BAX and increased cleavage of caspase-1, and GSDMD in HCT116 cells. Therefore, our results showed that PI3K/AKT was likely an upstream regulator of caspase-1 mediated GSDMD activation. Meanwhile, whether the inhibition of PI3K/AKT signaling is directly related to caspase activation remains to be further investigated.

Many studies have confirmed that ROS induced by SDG is critical for its therapeutic effect on cancer (Bowers et al., 2019; Li et al., 1999; Pietrofesa et al., 2016; Tannous et al., 2020). Consistently, our study confirmed that SDG administration may lead to the activation of the ROS, which in turn causing BAX–caspase–GSDMD signal axis mediated pyroptosis in CRC cells. Moreover, we also proved that NAC (a ROS scavenger) reversed the SDG-induced pyroptosis induction and suppression of p-AKT in HCT116 cells. However, ROS generation was not significantly affected by the PI3K/AKT pathway inhibitor, implying that ROS is a regulator of PI3K/AKT signaling. In addition, it was demonstrated that SDG inhibited PI3K/AKT signaling pathway for pyroptosis induction. Based on these data, our study concluded that SDG induced pyroptosis through BAX –caspase–GSDMD pathway in CRC cells via the ROS/PI3K/AKT signaling. Lastly, mechanistic experiments in nude mice further demonstrated that SDG showed satisfactory antitumor activity, as proved by tumor growth and immunohistochemistry assay. In vivo, SDG significantly promotes the cleavage of GSDMD and inhibits tumor growth and the expression of phosphorylated AKT. These data indicate that SDG may promote the activation of the caspase1-GSDMD canonical pyroptosis pathway by inhibiting PI3K/AKT signaling and exert its anticancer properties on CRC.

5 | CONCLUSIONS

This study found that SDG, a potential anticancer agent isolated from flaxseed, significantly inhibited CRC in vitro and in vivo by affecting the canonical pathway mediated by caspase-1. We further investigated the underlying molecular mechanism and found that the pro-pyroptosis activity of SDG is closely related to its ability to stimulate ROS production, inhibit PI3K/AKT activation, and activate BAX-mitochondrial intrinsic apoptotic pathway.

AUTHOR CONTRIBUTIONS

Hai Li and Zhen Wang participated in the design of the study. Tuo Chen, Zhen Wang, Lijun Zhang, Xianfei Zhong, and Jing Wang performed the experiments, analyzed the data, and wrote the manuscript. All authors read and approved the final manuscript.

ACKNOWLEDGMENTS

The present study was supported by the National Natural Science Foundation of China (Grant Numbers 81960526) and Natural Science Foundation of Ningxia Province (Grant Numbers 2019AAC03202).

CONFLICTS OF INTEREST

The authors declare no conflicts of interest.

DATA AVAILABILITY STATEMENT

The analyzed data sets generated during the present study are available from the corresponding author on reasonable request.

ORCID

Hai Li http://orcid.org/0000-0002-3584-8277

REFERENCES

Amable, L. (2016). Cisplatin resistance and opportunities for precision medicine. *Pharmacological Research*, *106*, 27–36. https://doi.org/10.1016/j.phrs.2016.01.001

Andersen, S. E., Andersen, I. B., Jensen, B. V., Pfeiffer, P., Ota, T., & Larsen, J. S. (2019). A systematic review of observational studies of trifluridine/tipiracil (TAS-102) for metastatic colorectal cancer. *Acta Oncologica*, *58*(8), 1149–1157. https://doi.org/10.1080/0284186x.2019.1605192

Bergsbaken, T., Fink, S. L., & Cookson, B. T. (2009). Pyroptosis: Host cell death and inflammation. *Nature Reviews Microbiology*, *7*(2), 99–109. https://doi.org/10.1038/nrmicro2070

Bowers, L. W., Lineberger, C. G., Ford, N. A., Rossi, E. L., Punjala, A., Camp, K. K., Kimler, B. K., Fabian, C. J., & Hursting, S. D. (2019). The flaxseed lignan secoisolariciresinol diglucoside decreases local inflammation, suppresses NFκB signaling, and inhibits mammary tumor growth. *Breast Cancer Research and Treatment*, *173*(3), 545–557. https://doi.org/10.1007/s10549-018-5021-6

Brown, J. S., & Banerji, U. (2017). Maximising the potential of AKT inhibitors as anti-cancer treatments. *Pharmacology and Therapeutics*, *172*, 101–115. https://doi.org/10.1016/j.pharmthera.2016.12.001

Casson, C. N., Yu, J., Reyes, V. M., Taschuk, F. O., Yadav, A., Copenhaver, A. M., Nguyen, H. T., Collman, R. G., & Shin, S. (2015). Human caspase-4 mediates noncanonical inflammasome activation against gram-negative bacterial pathogens. *Proceedings of the National Academy of Sciences of the United States of America*, *112*(21), 6688–6693. https://doi.org/10.1073/pnas.1421699112

Chen, W., Zheng, R., Baade, P. D., Zhang, S., Zeng, H., Bray, F., Jemal, A., Yu, X. Q., & He, J. (2016). Cancer statistics in China, 2015. *CA: A Cancer Journal for Clinicians*, *66*(2), 115–132. https://doi.org/10.3322/caac.21338

Chikara, S., Lindsey, K., Dhillon, H., Mamidi, S., Kittilson, J., Christofidou-Solomidou, M., & Reindl, K. M. (2017). Enterolactone induces G(1)-phase cell cycle arrest in nonsmall cell lung cancer cells by downregulating cyclins and cyclin-dependent kinases. *Nutrition and Cancer*, *69*(4), 652–662. https://doi.org/10.1080/01635581.2017.1296169

Danbara, N., Yuri, T., Tsujita-Kyutoku, M., Tsukamoto, R., Uehara, N., & Tsubura, A. (2005). Enterolactone induces apoptosis and inhibits growth of Colo 201 human colon cancer cells both in vitro and in vivo. *Anticancer Research*, *25*(3b), 2269–2276.

Ding, J., Wang, K., Liu, W., She, Y., Sun, Q., Shi, J., Sun, H., Wang, D. C., & Shao, F. (2016). Pore-forming activity and structural autoinhibition of the gasdermin family. *Nature*, *535*(7610), 111–116. https://doi.org/10.1038/nature18590

Fang, Y., Tian, S., Pan, Y., Li, W., Wang, Q., Tang, Y., Yu, T., Wu, X., Shi, Y., Ma, P., & Shu, Y. (2020). Pyroptosis: A new frontier in cancer. *Biomedicine & Pharmacotherapy = Biomédecine & Pharmacothérapie*, *121*, 109595. https://doi.org/10.1016/j.biopha.2019.109595

Feng, S., Fox, D., & Man, S. M. (2018). Mechanisms of gasdermin family members in inflammasome signaling and cell death. *Journal of Molecular Biology*, *430*(18, Pt B), 3068–3080. https://doi.org/10.1016/j.jmb.2018.07.002

Fink, S. L., & Cookson, B. T. (2006). Caspase-1-dependent pore formation during pyroptosis leads to osmotic lysis of infected host macrophages. *Cellular Microbiology*, *8*(11), 1812–1825. https://doi.org/10.1111/j.1462-5822.2006.00751.x

Gao, J., Qiu, X., Xi, G., Liu, H., Zhang, F., Lv, T., & Song, Y. (2018). Downregulation of GSDMD attenuates tumor proliferation via the intrinsic mitochondrial apoptotic pathway and inhibition of EGFR/Akt signaling and predicts a good prognosis in non-small cell lung cancer. *Oncology Reports*, *40*(4), 1971–1984. https://doi.org/10.3892/or.2018.6634

Global Burden of Disease Cancer, Collaboration, Fitzmaurice, C., Allen, C., Barber, R. M., Barregard, L., Bhutta, Z. A., Brenner, H., Dicker, D. J., Chimed-Orchir, O., Dandona, R., Dandona, L., Fleming, T., Forouzanfar, M. H., Hancock, J., Hay, R. J., Hunter-Merrill, R., Huynh, C., Hosgood, H. D., Johnson, C. O., … Rana, S. M. (2017). Global, regional, and national cancer incidence, mortality, years of life lost, years lived with disability, and disability-adjusted life-years for 32 cancer groups, 1990–2015: A systematic analysis for the Global Burden of Disease Study. *JAMA Oncol*, *3*(4), 524–548. https://doi.org/10.1001/jamaoncol.2016.5688

Heilig, R., Dilucca, M., Boucher, D., Chen, K. W., Hancz, D., Demarco, B., Shkarina, K., & Broz, P. (2020). Caspase-1 cleaves Bid to release mitochondrial SMAC and drive secondary necrosis in the absence of GSDMD. *Life Sci Alliance*, *3*(6). https://doi.org/10.26508/lsa.202000735

Hou, J., Zhao, R., Xia, W., Chang, C. W., You, Y., Hsu, J. M., Nie, L., Chen, Y., Wang, Y. C., Liu, C., Wang, W. J., Wu, Y., Ke, B., Hsu, J. L., Huang, K., Ye, Z., Yang, Y., Xia, X., Li, Y., … Hung, M. C. (2020). Author correction: PD-L1-mediated gasdermin C expression switches apoptosis to pyroptosis in cancer cells and facilitates tumour necrosis. *Nature Cell Biology*, *22*(11), 1396. https://doi.org/10.1038/s41556-020-00599-1

Jenab, M., & Thompson, L. U. (1996). The influence of flaxseed and lignans on colon carcinogenesis and beta-glucuronidase activity. *Carcinogenesis*, *17*(6), 1343–1348. https://doi.org/10.1093/carcin/17.6.1343

Jorgensen, I., & Miao, E. A. (2015). Pyroptotic cell death defends against intracellular pathogens. *Immunological Reviews*, *265*(1), 130–142. https://doi.org/10.1111/imr.12287

Kezimana, P., Dmitriev, A. A., Kudryavtseva, A. V., Romanova, E. V., & Melnikova, N. V. (2018). Secoisolariciresinol diglucoside of flaxseed and its metabolites: Biosynthesis and potential for nutraceuticals. *Frontiers in Genetics*, *9*, 641. https://doi.org/10.3389/fgene.2018.00641

Li, D., Yee, J. A., Thompson, L. U., & Yan, L. (1999). Dietary supplementation with secoisolariciresinol diglycoside (SDG) reduces experimental metastasis of melanoma cells in mice. *Cancer Letters*, *142*(1), 91–96. https://doi.org/10.1016/s0304-3835(99)00158-5

Lu, H., Zhang, S., Wu, J., Chen, M., Cai, M. C., Fu, Y., & Zhuang, G. (2018). Molecular targeted therapies elicit concurrent apoptotic and GSDME-dependent pyroptotic tumor cell death. *Clinical Cancer Research*, *24*(23), 6066–6077. https://doi.org/10.1158/1078-0432.Ccr-18-1478

Mármol, I., Sánchez-de-Diego, C., Pradilla Dieste, A., Cerrada, E., & Rodriguez Yoldi, M. J. (2017). Colorectal carcinoma: A general overview and future perspectives in colorectal cancer. *International Journal of Molecular Sciences*, *18*(1), 197. https://doi.org/10.3390/ijms18010197

Martinon, F., & Tschopp, J. (2005). NLRs join TLRs as innate sensors of pathogens. *Trends in Immunology*, *26*(8), 447–454. https://doi.org/10.1016/j.it.2005.06.004

Martinon, F., & Tschopp, J. (2007). Inflammatory caspases and inflammasomes: Master switches of inflammation. *Cell Death and Differentiation*, *14*(1), 10–22. https://doi.org/10.1038/sj.cdd.4402038

McQuade, R. M., Stojanovska, V., Bornstein, J. C., & Nurgali, K. (2017). Colorectal cancer chemotherapy: The evolution of treatment and new approaches. *Current Medicinal Chemistry*, *24*(15), 1537–1557. https://doi.org/10.2174/0929867324666170111152436

Miao, E. A., Rajan, J. V., & Aderem, A. (2011). Caspase-1-induced pyroptotic cell death. *Immunological Reviews*, *243*(1), 206–214. https://doi.org/10.1111/j.1600-065X.2011.01044.x

Ouyang, L., Shi, Z., Zhao, S., Wang, F. T., Zhou, T. T., Liu, B., & Bao, J. K. (2012). Programmed cell death pathways in cancer: A review of apoptosis, autophagy and programmed necrosis. *Cell Proliferation*, *45*(6), 487–498. https://doi.org/10.1111/j.1365-2184.2012.00845.x

Pei, Q., Liu, G. S., Li, H. P., Zhang, Y., Xu, X. C., Gao, H., Zhang, W., & Li, T. (2019). Long noncoding RNA SNHG14 accelerates cell proliferation, migration, invasion and suppresses apoptosis in colorectal cancer cells by targeting miR-944/KRAS axis through PI3K/AKT pathway. *European Review for Medical and Pharmacological Sciences*, *23*(22), 9871–9881. https://doi.org/10.26355/eurrev_201911_19551

Pietrofesa, R. A., Velalopoulou, A., Albelda, S. M., & Christofidou-Solomidou, M. (2016). Asbestos induces oxidative stress and activation of Nrf2 signaling in murine macrophages: Chemopreventive role of the synthetic lignan secoisolariciresinol diglucoside (LGM2605). *International Journal of Molecular Sciences*, *17*(3), 322. https://doi.org/10.3390/ijms17030322

Pilar, B., Güllich, A., Oliveira, P., Ströher, D., Piccoli, J., & Manfredini, V. (2017). Protective role of flaxseed oil and flaxseed lignan secoisolariciresinol diglucoside against oxidative stress in rats with metabolic syndrome. *Journal of Food Science*, *82*(12), 3029–3036. https://doi.org/10.1111/1750-3841.13964

Rom, S., Zuluaga-Ramirez, V., Reichenbach, N. L., Erickson, M. A., Winfield, M., Gajghate, S., Christofidou-Solomidou, M., Jordan-Sciutto, K. L., & Persidsky, Y. (2018). Secoisolariciresinol diglucoside is a blood-brain barrier protective and anti-inflammatory agent: Implications for neuroinflammation. *Journal of Neuroinflammation*, *15*(1), 25. https://doi.org/10.1186/s12974-018-1065-0

Shi, J., Zhao, Y., Wang, K., Shi, X., Wang, Y., Huang, H., Zhuang, Y., Cai, T., Wang, F., & Shao, F. (2015). Cleavage of GSDMD by inflammatory caspases determines pyroptotic cell death. *Nature*, *526*(7575), 660–665. https://doi.org/10.1038/nature15514

Siegel, R. L., Miller, K. D., & Jemal, A. (2018). Cancer statistics, 2018. *CA: A Cancer Journal for Clinicians*, *68*(1), 7–30. https://doi.org/10.3322/caac.21442

Sieminska, I., & Baran, J. (2020). Myeloid-derived suppressor cells in colorectal cancer. *Frontiers in Immunology*, *11*, 1526. https://doi.org/10.3389/fimmu.2020.01526

Silveira, T. N., & Zamboni, D. S. (2010). Pore formation triggered by *Legionella* spp. is an Nlrc4 inflammasome-dependent host cell response that precedes pyroptosis. *Infection and Immunity*, *78*(3), 1403–1413. https://doi.org/10.1128/iai.00905-09

Song, M., Bode, A. M., Dong, Z., & Lee, M. H. (2019). AKT as a therapeutic target for cancer. *Cancer Research*, *79*(6), 1019–1031. https://doi.org/10.1158/0008-5472.Can-18-2738

Takagi, A., Kano, M., & Kaga, C. (2015). Possibility of breast cancer prevention: Use of soy isoflavones and fermented soy beverage produced using probiotics. *International Journal of Molecular Sciences*, *16*(5), 10907–10920. https://doi.org/10.3390/ijms160510907

Tannous, S., Haykal, T., Dhaini, J., Hodroj, M. H., & Rizk, S. (2020). The anti-cancer effect of flaxseed lignan derivatives on different acute myeloid leukemia cancer cells. *Biomedicine & Pharmacotherapy = Biomédecine & Pharmacothérapie*, *132*, 110884. https://doi.org/10.1016/j.biopha.2020.110884

Tsuchiya, K. (2021). Switching from apoptosis to pyroptosis: Gasdermin-elicited inflammation and antitumor immunity. *International Journal of Molecular Sciences*, *22*(1), 426. https://doi.org/10.3390/ijms22010426

Viganò, E., Diamond, C. E., Spreafico, R., Balachander, A., Sobota, R. M., & Mortellaro, A. (2015). Human caspase-4 and caspase-5 regulate the one-step non-canonical inflammasome activation in monocytes. *Nature Communications*, *6*, 8761. https://doi.org/10.1038/ncomms9761

Wallach, D., Kang, T. B., Dillon, C. P., & Green, D. R. (2016). Programmed necrosis in inflammation: Toward identification of the effector molecules. *Science*, *352*(6281), aaf2154. https://doi.org/10.1126/science.aaf2154

Wang, Y. Y., Liu, X. L., & Zhao, R. (2019). Induction of pyroptosis and its implications in cancer management. *Frontiers in Oncology*, *9*, 971. https://doi.org/10.3389/fonc.2019.00971

Wei, Z., Nie, G., Yang, F., Pi, S., Wang, C., Cao, H., Guo, X., Liu, P., Li, G., Hu, G., & Zhang, C. (2020). Inhibition of ROS/NLRP3/Caspase-1 mediated pyroptosis attenuates cadmium-induced apoptosis in duck renal tubular epithelial cells. *Environmental Pollution*, *273*, 115919. https://doi.org/10.1016/j.envpol.2020.115919

Woo, Y., Lee, H. J., Jung, Y. M., & Jung, Y. J. (2020). Regulated necrotic cell death in alternative tumor therapeutic strategies. *Cells*, *9*(12), 2709. https://doi.org/10.3390/cells9122709

Wu, L. S., Liu, Y., Wang, X. W., Xu, B., Lin, Y. L., Song, Y., & Li, B. H. (2020). LPS enhances the chemosensitivity of oxaliplatin in HT29 cells via GSDMD-mediated pyroptosis. *Cancer Management and Research*, *12*, 10397–10409. https://doi.org/10.2147/cmar.S244374

Xi, H., Zhang, Y., Xu, Y., Yang, W. Y., Jiang, X., Sha, X., & Wang, H. (2016). Caspase-1 inflammasome activation mediates homocysteine-induced pyrop-apoptosis in endothelial cells. *Circulation Research*, *118*(10), 1525–1539. https://doi.org/10.1161/circresaha.116.308501

Yao, W., Lin, Z., Shi, P., Chen, B., Wang, G., Huang, J., Sui, Y., Liu, Q., Li, S., Lin, X., Liu, Q., & Yao, H. (2020). Delicaflavone induces ROS-mediated apoptosis and inhibits PI3K/AKT/mTOR and Ras/MEK/Erk signaling pathways in colorectal cancer cells. *Biochemical Pharmacology*, *171*, 113680. https://doi.org/10.1016/j.bcp.2019.113680

Zhang, J., Wang, X., Vikash, V., Ye, Q., Wu, D., Liu, Y., & Dong, W. (2016). ROS and ROS-mediated cellular signaling. *Oxidative Medicine and Cellular Longevity*, *2016*, 4350965. https://doi.org/10.1155/2016/4350965

Zhang, Y., Li, F., Wang, L., & Lou, Y. (2021). A438079 affects colorectal cancer cell proliferation, migration, apoptosis, and pyroptosis by inhibiting the P2X7 receptor. *Biochemical and Biophysical Research Communications*, *558*, 147–153. https://doi.org/10.1016/j.bbrc.2021.04.076

Zhao, Y., Hu, X., Liu, Y., Dong, S., Wen, Z., He, W., Zhang, S., Huang, Q., & Shi, M. (2017). ROS signaling under metabolic stress: Cross-talk between AMPK and AKT pathway. *Molecular Cancer*, *16*(1), 79. https://doi.org/10.1186/s12943-017-0648-1

Zheng, Z., & Li, G. (2020). Mechanisms and therapeutic regulation of pyroptosis in inflammatory diseases and cancer. *International Journal of Molecular Sciences*, *21*(4), 1456. https://doi.org/10.3390/ijms21041456

How to cite this article: Chen, T., Wang, Z., Zhong, J., Zhang, L., Zhang, H., Zhang, D., Xu, X., Zhong, X., Wang, J., & Li, H. (2022). Secoisolariciresinol diglucoside induces pyroptosis by activating caspase-1 to cleave GSDMD in colorectal cancer cells. *Drug Development Research*, 83, 1152–1166. https://doi.org/10.1002/ddr.21939